

Computational Study of Thermal Rectification from Nanostructured Interfaces

N.A. Roberts

Department of Mechanical Engineering
Vanderbilt University
Nashville, TN USA, 37325
nicholas.roberts@vanderbilt.edu

D.G. Walker

Department of Mechanical Engineering
Vanderbilt University
Nashville, TN USA, 37325
greg.walker@vanderbilt.edu

ABSTRACT

Thermal rectification is a phenomenon in which transport is preferred in one direction over the opposite. Though observations of thermal rectification have been elusive, it could be useful in many applications such as thermal management of electronics and improvement of thermoelectric devices. The current work explores the possibility of thermally rectifying devices with the use of nanostructured interfaces. Interfaces can theoretically result in thermally rectifying behavior because of the difference in phonon frequency content between two dissimilar materials. The current work shows an effective rectification of greater than 25% in a device composed of two different materials divided equally by a single planar interface.

Keywords: thermal rectification, molecular dynamics, interface conductance

Nomenclature

A	area (m^2)
c_v	specific heat ($\text{J kg}^{-1} \text{K}^{-1}$)
g	spring constant (kg s^{-2})
l	mean free path (m)
m	atomic mass (kg)
q	heat transfer (W)
r	atomic displacement (m)
T	temperature (K)
U	interatomic potential (J)
v	phonon velocity (m s^{-1})
x	device location (m)
ε	depth of L-J potential well (J)
ξ	effective rectification
k	thermal conductivity ($\text{W m}^{-1} \text{K}^{-1}$)
ω	phonon frequency (rad s^{-1})
σ	zero potential distance (m)

1 Introduction

Thermal rectification is a phenomenon where the magnitude of transport in a specific direction through a material is dependent on the sign or direction of the temperature gradient, and though observations of the effect in solids have been rare, rectifying behavior could have widespread applications. Records of rectification date back as early as 1935 when Starr [1] found that copper/cuprous oxide systems showed thermal as well as electrical rectification. Walker [2] reviewed several candidate theoretical models based on geometric asymmetries with unequal thermal expansion and offered several alternative explanations for rectification behavior based on non-equilibrium effects. Examples of these models include lattice vibrations, which reflect differently depending on the geometry and characteristics of the structure or transmission across an interface. These theories suggest that rectification could be exploited with our improved ability to manipulate materials at the nanoscale. In 2002 Terraneo et al. [3] demonstrated theoretical rectification behavior using a nonlinear one-dimensional chain of atoms between two thermostats at different temperatures. In their system, Terraneo was able to change the chain from a normal conductor in one direction to a nearly perfect insulator in the other direction due to the non-linearity of the potential. In a similar study in 2004, Li et al. [4] simulated a nonlinear lattice and calculated a difference in conduction between

the two directions to be 100 times that of Terraneo [3]. In 2006 Chang et al. [5] suggested solitons could be responsible for rectification and showed experimentally that greater conduction resulted in the direction of decreasing mass density in an engineered material having a non-uniform mass distribution along nanotubes. The non-uniform mass distribution was obtained by depositing $C_9H_{16}Pt$ with a much higher concentration at one end of the nanotube than the other. Recently other asymmetric nanoscale structures including voids and inclusions have been examined as possible rectifying mechanisms [6]. For a complete review of thermal rectification observations in solid systems please refer to [7].

The current work involves a molecular dynamics study of the rectification effects of a single interface within a thin film. The inspiration for this work came from Walker 2006 [2], which proposed a possible model for rectification due to phonon scattering at interfaces. The effects of a pristine interface should be different than that of a rough or asymmetric interface. In this work we have compared the perfect interface to rough interfaces by varying the degree of roughness and asymmetry of the interfaces. The goal of the molecular dynamics work is to show theoretical evidence of the existence of thermal rectification due to the difference in phonon transmission between two different materials due to a difference in material properties, specifically frequency content, and to explain how scattering at fabricated interfaces results in our limited ability to measure thermally rectifying behavior experimentally. Currently there exist several other studies that use non-equilibrium molecular dynamics to investigate thermal rectification in interfacial systems [8].

2 Approach

The devices studied using molecular dynamics are half argon and half krypton (excluding the ellipsoidal interface) with a single interface located at the center. The types of interfaces investigated include perfect interfaces, rough interfaces and asymmetric interfaces, each of which is shown in Fig. 1.

An FCC crystalline lattice is assumed with a Lennard-Jones inter-atomic potential given as

$$U(r) = 4\epsilon \left[\left(\frac{\sigma}{r} \right)^{12} - \left(\frac{\sigma}{r} \right)^6 \right]. \quad (1)$$

The properties of argon and krypton are given in Table 1.

XMD, an open source, general purpose molecular dynamics code [9] and LAMMPS, another open source, general purposed molecular dynamics code [10] are used for the computations in this work. Small modifications were made to the code to extract the information necessary to calculate the thermal conductivity of the device by recording the energy added and subtracted to each constant temperature bath throughout the simulation. The LAMMPS package was used to verify the results of the XMD package and to speedup calculations due to its parallel computing capabilities. The system is composed

of 6 unit cells (3 on each side) of wall where the atom positions are fixed, 8 unit cells (4 on each side) for the high (60 K) and low (40 K) fixed temperature baths and a varying number of unit cells for the simulation domain where the interface is located. The cross-sectional area of these systems was 64 square unit cells (8×8). This configuration was used because 4 planes of fixed atoms at the ends of the device are sufficient to perform non-equilibrium molecular dynamics with the Lennard-Jones potential because of the short range of the inter-atomic potential [11]. The interfaces studied in this work include a perfect interface where the two constituent materials are perfectly divided at the center of the device, a rough or diffused interface where the two constituent materials have atoms on both sides of the interface with two different levels of diffusion and two asymmetric interfaces, which include hemispherical and ellipsoidal geometries. These interfaces were created using a MATLAB script to place the correct atom type on the chosen side of the interface to form the desired geometry. These systems were studied at a range of average system temperatures.

The first step in this work was to determine a simulation box size to be fixed and maintained throughout the simulation. To calculate this box size, the temperature gradient was imposed and the device was allowed to relax to minimize the strain on the system. The simulation was then initialized using the calculated box size at a temperature of 50 K and allowed to run to 5000 time steps with a $\Delta t = 3.2 \times 10^{-15}$ s. The temperature gradient is then applied, and the simulation is allowed to run for an additional 195,000 to 1,995,000 time steps (depending on device size) which is a total simulation time of 0.64 ns to 6.4 ns. Throughout the simulation the energy added and subtracted to and from each constant temperature bath is recorded. During the early stages of the simulation the average energy fluctuates rapidly. After which the average reaches a near constant value. At this point the simulation is at steady-state and the energy added to the high temperature bath is equal to that of the energy subtracted from the low temperature bath. This amount of energy added or subtracted is the total heat transfer of the system at the given temperature difference of 20 K. With the computed flux, the effective thermal conductivity is then calculated using Fourier's law for steady conduction,

$$k = -\frac{q \Delta x}{A \Delta T}, \quad (2)$$

where Δx is the domain length between the baths, and A is the cross sectional area of the film as simulated. Fourier's law is a phenomenological law where the thermal conductivity is considered a proportionality constant or "effective" property. In the current work we calculate and record the energy required to maintain fixed temperatures at each bath. This energy is then divided by the time step to obtain the heat transfer q in equation 2. Since all other values in equation 2 are fixed and the heat transfer is averaged over long times, Fourier's law provides an effective conductivity for the device [11].

In all simulations a fixed mass ratio of argon and krypton are maintained except for the ellipsoidal interface. To evaluate

the rectifying behavior of the interfaces we will now introduce a parameter ξ , which is defined as

$$\xi = \frac{k_{Ar-Kr} - k_{Kr-Ar}}{k_{Kr-Ar} + k_{Ar-Kr}}, \quad (3)$$

where k_{Ar-Kr} and k_{Kr-Ar} are the thermal conductivities from the hot argon to cold krypton and hot krypton to cold argon baths, respectively. A value of $\xi = 0$ means there is no difference when the temperature gradient is reversed and therefore no rectification; a value of $\xi = 1$ means the system is an ideal thermal rectifier. The error bars in the data were calculated based on the fluctuation of the average temperature of the baths and the energy added and subtracted from the baths to maintain the bath temperature.

3 Results

In this work we have investigated thermally rectifying behavior in devices with interfaces. The effects of device length, temperature and scattering will be investigated systematically in each of the subsequent sections.

The first step in this work was to verify and validate the molecular dynamics code used for the calculation of thermally rectifying behavior. Simulations of pure argon are fit to a kinetic theory and compared to reported experimental measurements. The simulated conductivity data reported in Fig. 2 were calculated using equation 2 with the baths held constant at 60 K and 40 K, respectively. The theoretical conductivity is given from kinetic theory as

$$k = \frac{1}{3} c_v v l_d, \quad (4)$$

where l_d is the phonon mean free path of the device. In the limit of large devices, the mean free path is governed by phonon-phonon scattering. For small devices, the boundary scattering becomes significant such that

$$\frac{1}{l_d} = \frac{1}{l_{p-p}} + \frac{1}{l_B}, \quad (5)$$

where l_B is simply the device size and l_{p-p} represents the inherent phonon-phonon scattering mean free path. The thermal conductivity as a function of device length is derived using experimental values of $c = 22 \text{ J/mol}$ [12] and $v = (v_l + 2v_t)/3$, where $v_l = 1500 \text{ m/s}$ and $v_t = 841 \text{ m/s}$ are the longitudinal and transverse velocities respectively [13]. The kinetic theory

model appears to match the molecular dynamics data quite well. The inset of Fig. 2 shows the inverse conductivity as a function of inverse length, which is how the infinite length thermal conductivity $k_d = 0.51 \text{ W/mK}$ is determined.

Experimental values for solid argon vary from $k = 0.46 \text{ W/mK}$ [14] to $k = 0.55 \text{ W/mK}$ [15], so our value of $k_{\text{XMD}} = 0.51 \text{ W/mK}$ is easily in line with measured values for single crystals. Moreover, the estimated bulk mean-free path of $l_{\text{bulk}} = 2.9 \text{ nm}$ compares favorably to [16]. Similarly, at 40 K the mean free path of phonons in pure argon is 3.4 nm while at 10 K the mean free path is 12.2 nm [17], which also correspond well with our own simulations. Based on the simulation data, not only has the correct value of bulk thermal conductivity been recovered, but also the value appears consistent as the device size changes. For smaller devices the finite-size effect reduces the effective conductivity because only certain vibrational modes are available for transport and because of increased boundary scattering [18, 19]. This effect has provided the impetus to study nanostructured devices for thermoelectric performance [20]. Fig. 3 shows the temperature distribution through a device with the imposed temperature baths, which is relatively linear [21]. The plot shows the variation in the measured temperature, which is the source of the error bars in the conductivity plots.

The device length plays an extremely important role on the thermal conductivity, therefore we expect it to have an impact on the level of thermal rectification as well. From our simulation data, presented in Fig. 4, little to no rectification appears at small device lengths, but increases with device size. Four possible mechanisms to explain the results will be discussed.

The first mechanism to explain the observations is simply a bulk argument provided by Dames [22] and refined by Go [23] for two materials with varying thermal conductivities. If the thermal conductivity of each layer varies differently in temperature, rectification is possible. The overall thermal conductivity is a combination of the conductivities of each layer at their respective temperatures. When the gradient is reversed, the thermal conductivity of one material decreases much more than the other increases giving rise to net increase or decrease in thermal conductivity overall. In molecular dynamics simulations, we apply unusually large temperature gradients to reduce the noise in the simulation. Therefore, the temperature on each side of the interface can be at significantly different temperatures, which amplifies the effect.

Although experimental data are scarce and MD data are too noisy to test this argument rigorously, the bulk hypothesis would support the fact that little rectification is observed at small lengths. The thermal conductivity at reduced scales is primarily a function of the boundary scattering, which is the same in each layer, so the variation in conductivity as a function of temperature is reduced. However, at longer lengths, where temperature dependent mean-free paths dominate the thermal conductivity, temperature can have a significant effect on the results. For high-temperature regions, above 10 K in our case, the temperature-dependent conductivity can be fit to a power-law expression, $k(T) = k_o T^n$. From the limited data of bulk argon [24] and krypton [25], the exponent of argon is approximated as $n = -1.3$ in the region from 10 K to 70 K. In that same region, the exponent for krypton is $n = -1.2$. The difference in exponents suggests the possibility of rectification. Using these values, the amount of rectification can be predicted for an average increase of 1 K on the heated side and an average

decrease in the cooled side of 1 K. Fig. 5 shows that the potential for rectification is increased at lower temperatures because of bulk temperature effects. Of course the magnitude of rectification becomes greater with greater temperature differences.

The second mechanism that has been promoted to explain thermal rectification at interfaces is the mismatch of phonon spectra across the interface [8, 26]. Because argon is a lighter atom, its maximum frequency is larger than that of krypton. If the maximum frequencies are approximated as $\omega_{\max} \approx \sqrt{g/m}$ where g can be estimated by fitting the potential well with a parabola. The ratio of maximum frequencies $\sqrt{m_{\text{Kr}}/m_{\text{Ar}}} \approx 1.25$ is a result of the difference in atomic mass. Because of the difference in mass, the two materials will have a different dispersion and different frequency content. Krypton, because of its lower maximum frequency, will not be able to transmit the high-frequency phonons without inelastic scattering to lower-frequency phonons. When the temperature gradient favors heat transfer in the argon to krypton direction, the thermal conductivity will decrease because more higher energy states that can not transmit across the interface will populate the argon layer per the Bose-Einstein distribution. The result is a reduction in thermal conductivity in the argon to krypton direction. Otherwise, a gradient that favors the krypton to argon direction will populate high-energy states in the krypton that are still able to transmit from krypton to argon because argon can accept those frequencies without scattering inelastically at the boundary. Therefore, the conductivity remains largely unchanged. The net rectification due to this population of states is negative, which is contrary to the observations.

Although this explanation appears to violate the observations, this result has been seen elsewhere (without explanation) [16]. In Fig. 4 and 6 we see that the sign of rectification changes in the long device lengths. This change is a result of no inelastic scattering in the 10 K system and some inelastic scattering in the 50 K system. As we said in the last section, at low temperatures and longer device lengths the rectifying effect is due the existence of high frequency modes in the argon that are not allowed in the krypton which limits the ability for phonons to transmit from the argon to the krypton. At higher temperatures inelastic scattering begins to occur which allows the modes to transmit by scattering into multiple lower frequency modes. This allows the higher frequency modes in argon to contribute to the thermal transport through the system, but does not change the ability of the krypton to transmit greatly which is why we see the change in the sign of the level of rectification. In the limit of total inelastic scattering, such as in bulk systems and at higher temperatures, there would likely be no observable rectifying effect.

Now consider a device at very low temperatures. The effects of reduced temperature are two-fold. First, Umklapp scattering, which is a strong function of temperature is reduced. Without this inelastic mechanism, high-frequency phonons are not allowed to scatter into lower energy states. Therefore, the high frequency phonons in the argon, are less likely to decay into modes that are allowed to transmit into the krypton. However, the krypton modes do not need to rely on inelastic scattering to transmit into the argon. Therefore, the sign of the rectification should be negative as observed in Fig. 6 for longer devices. The low temperatures also have a second competing effect. At low temperatures, the higher-frequency modes tend

to get frozen out. If the argon contains very few high-frequency modes, then the phonon mismatch does not matter because the frequencies forbidden to transmit don't even exist. The reason the rectification transitions from negative to positive with decreasing length is because as the device size is reduced, the boundary scattering becomes dominant. Consequently, the inelastic scattering effect (negative rectification) is reduced, which allows the freeze-out effect (positive rectification) to become significant.

The third mechanism involves confinement. As device sizes are reduced, the largest phonon wavelength that is allowed to exist is half the device size (from boundary to interface). The dominant phonon wavelength is of the order of 2 – 3 nm at 70K, so confinement will not have a dramatic effect unless the device is incredibly small or the temperature is extremely low. The 16UC cases allow a maximum wavelength of $\lambda_{\max} = 4.24$ nm, so we might expect to see confinement effects starting in these devices and smaller devices. The results of confinement will be to limit both krypton and argon to higher frequency modes. However, the effect is more dramatic in argon because of its dispersion. Therefore, the direction of the rectification due to confinement is negative. Nevertheless, we do not observe direct evidence of confinement effects in our simulations.

We expect the rectifying effect to disappear as we increase the device length (as the actual phonon mean free path becomes much shorter than the distance between the constant temperature bath and the interface). In systems with longer device lengths each section will exhibit bulk properties (high levels of multi-phonon scattering) and the impact of the interface will become negligible in comparison. This reason, inelastic scattering, and our lack of a thorough investigation in these systems is why thermal rectification has not been observed in nanostructured interfaces at this time.

At low temperatures inelastic scattering does not typically occur in high quality or perfectly planar interfaces, which are described well by the AMM and DMM [27], but as the temperature of the interface increases it begins to play a major role in the interface conductance which is partially accounted for in the JFDMM [28]. Transport through perfect interfaces in this work is still not completely described by the AMM because of the lattice, or by the DMM because Debye ratio ($\sqrt{m_{Ar}/m_{Kr}}$) is greater than 0.6 [29] even at low temperatures.

Fig. 7 shows the level of rectification as a function of device temperature where we again see the impact of inelastic scattering on the sign of the level of rectification. In this figure we see a rectifying effect with the greater transport direction being from krypton to argon at low temperatures, a transition region where little or no rectification occurs at slightly higher temperatures, a region where the greater transport direction is argon to krypton at even higher temperatures and we begin to see a reduction in the level of rectification in a region of higher temperature. We were not able to increase the temperature of the simulations any higher because the bath temperatures were approaching the melting point of argon [30].

The fourth mechanism involves how the interface geometry affects the rectification. Interface scattering due to roughness also plays an important role in thermally rectifying devices composed of an interface between two different materials. When the quality of the interface is degraded or the size of interfacial region is increased more scattering occurs, which allows

phonons that were previously restricted to one side of the interface the opportunity to transmit at least partially. Similar to the effects of higher temperatures, the rough interfaces act to increase the probability of inelastic scattering by increasing the potential energy due to strain at the interface. Fig. 8 shows the effective rectification calculated from equation 3 for the perfect and imperfect interfaces as a function of the device length from the XMD package. The coarse and fine interfaces show less rectifying behavior presumably due to the increased scattering at the interface. Due to the considerable noise associated with molecular dynamics simulations (4.2% - 5.2%) because of temperature fluctuations and energy rescaling at the baths it is difficult to confirm our hypothesis. Although, one could argue that the results show that the perfect interface results in the greatest level of rectification. Fig. 9 shows the effective rectification of the asymmetric (hemispherical and ellipsoidal) interfaces as a function of device length along with the effective rectification of the perfect interface also from the XMD package. It appears from these results that the asymmetric interfaces degrade the rectifying effect because the amount of rectification is comparable to what is seen in the rough interfaces due to increased scattering at the interface.

We again repeat some of these simulations with the LAMMPS package. Since the asymmetric interfaces have the same impact on the rectification effect as the rough interfaces we have decided not to continue with those interfaces. Future simulations could be performed when much larger systems can be studied where the asymmetric nature of the interface can be accurately represented in the simulation. We have designed two new rough interfaces which resemble the diffusion of atoms at an interface with two different levels or sizes of the diffusion region. Fig. 10 shows the level of rectification calculated as a function of temperature for the rough interfaces along with the values obtained from the perfect planar interface. In this figure we see the levels of rectification maintain the same trend as in the perfect interface case (Fig. 7), but to a greatly decreased level. These levels all fall within 5% of no rectification which is within the noise of the simulation which means we can not determine whether rectification is occurring at these interfaces, but we note that the rectification observed in the perfect planar interface is greater and has been shown to exist. Based on this observation we can infer that the elimination of the rectifying effect shown here is a result of increased inelastic scattering which eliminates the asymmetric phonon transport at the interface. These results show good agreement with the results of phonon wave-packet simulations in [26]. These results showed an increase in rectification with the addition of an interface roughness while the current results do not. This difference is seen because of the relative size of the interface in the two systems. The current system has a relatively large interface region in comparison to the entire system (1-5 of the up to 150 unit cells) while the wave-packet systems have a relatively small interface (1-5 of the 1000 unit cells). This difference shows that with some inelastic scattering occurring at the interface we expect to see an increase in the level of rectification while in the current systems investigated with non-equilibrium molecular dynamics we are unable to see the transition with such accuracy. Larger systems could be investigated in the future to show this effect.

4 Conclusions

In the present work, molecular dynamics results showed that thermal rectification is theoretically possible and the effect is reduced as the quality of the interface is degraded with the addition of somewhat randomly distributed atoms of each of the constituent materials at the interface. A reduction in rectification from the perfect interface was also seen with the introduction of the asymmetric interfaces. The molecular dynamics results suggest that the reason thermal rectification is not observed in many cases is due to the poor quality of interfaces in devices consisting of two different materials. In this work we have observed that thermal transport is preferred in the direction of higher mass and softer potential to lower mass and stiffer potential. This effect is due to the difference in frequency content between the constituent materials and the transmission of those frequencies across the interface. As the interface is degraded inelastic scattering will increase resulting in no rectification. In the case of the perfect interface, the acoustic mismatch model, which ignores scattering and results in maximum rectification, can be used to approximate the level of rectification by including frequency-dependent coefficients. As the temperature increases or the surface is degraded the diffuse mismatch model will apply where scattering then occurs as a result of the diffusion of materials at the interface, and the difference in transmission becomes related to the difference in the phonon density of states between the two materials assuming all diffuse scattering is elastic. When inelastic scattering is dominant at the interface, the phonon transmission dependence on frequency is reduced and no rectification will be observed.

These findings suggest that new materials can be used to provide advanced passive thermal control of localized transport by exploiting nanotechnology. If no scattering occurs at the interface (low temperature and planar interface) the magnitude of the rectification should be related to the ratio of maximum allowable phonon frequencies of the two materials. If only elastic scattering occurs at the interface (planar interface) the magnitude of the rectification should be related to the ratio of the phonon density of states of the two materials. At higher temperature and/or level of degradation of the interface, inelastic scattering will dominate and mitigate any thermally rectifying behavior. These mechanisms essentially result in a reduction of transport compared to the bulk material. Therefore these mechanisms cannot in general be used to improve transport favorably in a given direction; they can only be used to reduce transport in a given direction.

Acknowledgments

The authors would like to thank DARPA for funding this project and Chris Dames at UC Riverside for his useful conversations/papers.

References

- [1] Starr, C., 1935. "The copper oxide rectifier". *Physics (Journal of Applied Physics)*, **7**, Jan., pp. 15–19.

- [2] Walker, D. G., 2006. “Thermal rectification mechanisms including noncontinuum effects”. In proceedings of the Joint ASME-ISHMT Heat Transfer Conference.
- [3] Terraneo, M., Peyrard, M., and Casati, G., 2002. “Controlling the energy flow in non-linear lattices: A model for a thermal rectifier”. *Physical Review Letters*, **88**(9), Mar., pp. 4302.1–4302.4.
- [4] Li, B., Wang, L., and Casati, G., 2004. “Thermal diode: Rectification of heat flux”. *Physical Review Letters*, **93**(18), Mar., pp. 4301.1–4301.4.
- [5] Chang, C. W., Okawa, D., Majumdar, A., and Zettl, A., 2006. “Solid-state thermal rectifier”. *Science*, **314**, Nov., pp. 1121–1124.
- [6] Miller, J., Jang, W., and Dames, C., 2009. “Thermal rectification by ballistic phonons in asymmetric nanostructures”. In Proceedings of the ASME 2009 Heat Transfer Summer Conference.
- [7] Roberts, N., and Walker, D., in press. “A review of thermal rectification observations and mechanisms in solid materials”. *International Journal of Thermal Sciences*.
- [8] Wang, S.-C., and Liang, X.-G., 2011. “Investigation of thermal rectification in bi-layer nanofilm by molecular dynamics”. *International Journal of Thermal Sciences*, in press.
- [9] Rifkin, J. XMD - molecular dynamics program. <http://xmd.sourceforge.net/doc/manual/xmd.html>.
- [10] Plimpton, S. LAMMPS - large-scale atomic/molecular massivley pallel simulator. <http://lammps.sandia.gov/>.
- [11] Lukes, J. R., Li, D., Liang, X.-G., and Tien, C.-L., 2000. “Molecular dynamics study of solid thin-film thermal conductivity”. *Journal of Heat Transfer*, **122**(3), Aug., pp. 536–543.
- [12] Haenssler, F., Gamper, K., and Serin, B., 1970. “Constant-volume specific heat of solid argon”. *Journal of Low Temperature Physics*, **3**, pp. 23–28.
- [13] Keeler, G. J., and Batchelder, D. N., 1970. “Measurement of the elastic constants of argon from 3 to 77 degrees K”. *Journal of Physics C: Solid State Physics*, **3**(3), pp. 510–522.
- [14] Touloukian, Y., Liley, P., and Saxena, S., 1970. *Thermal Conductivity: Nonmetallic Liquids and Gases*. IFI/Plenum.
- [15] Christen, D. K., and Pollack, G. L., 1975. “Thermal conductivity of solid argon”. *Phys. Rev. B*, **12**(8), Oct., pp. 3380–3391.
- [16] Ju, S., and Liang, X., 2010. “Investigation of argon nanocrystalline thermal conductivity by molecular dynamics simulation”. *Journal of Applied Physics*, **108**(104307).
- [17] Choi, S.-H., Maruyama, S., Kim, K.-K., and Lee, J.-H., 2003. “Evaluation of the phonon mean free path in thin films by using classical molecular dynamics”. *Journal of Korean Physics Society*, **43**(5), pp. 747–753.
- [18] Mingo, N., and Broido, D. A., 2005. “Length dependence of carbon nanotube thermal conductivity and the “problem of long waves””. *Nano Letters*, **5**(7), June, pp. 1221–1225.

- [19] Schelling, P. K., Phillpot, S. R., and Keblinski, P., 2002. “Comparison of atomic-level simulation methods for computing thermal conductivity”. *Phys. Rev. B*, **65**(14), Apr., p. 144306.
- [20] Roberts, N., Li, D., and Walker, D., 2009. “Molecular dynamics simulation of thermal conductivity of nanocrystalline composite films”. *International Journal of Heat and Mass Transfer*, **52**(7–8), Mar., pp. 2002–2008.
- [21] McGaughey, A. J. H., and Kaviany, M., 2006. “Phonon transport in molecular dynamics simulations: Formulation and thermal conductivity prediction”. *Advances in Heat Transfer*, **39**, pp. 169–255.
- [22] Dames, C., 2009. “Solid-state thermal rectification with existing bulk materials”. *Journal of Heat Transfer*, **131**(6), p. 061301.
- [23] Go, D. B., and Sen, M., 2010. “On the condition for thermal rectification using bulk materials”. *Journal of Heat Transfer*, **132**(124502), Dec.
- [24] Clayton, F., and Batchelder, D. N., 1973. “Temperature and volume dependence of the thermal conductivity of solid argon”. *Journal of Physics C: Solid State Physics*, **6**(7), pp. 1213–1228.
- [25] Dudkin, V. V., Gorodilov, B. Y., Krivchikov, A. I., and Manzhelii, V. G., 2000. “Thermal conductivity of solid krypton with methane admixture”. *Low-Temperature Physics*, **26**(9–10), pp. 762–766.
- [26] Roberts, N., and Walker, D., 2010. “Phonon wave-packet simulations of Ar/Kr interfaces for thermal rectification”. *Journal of Applied Physics*, **108**(12), Dec., p. 123515.
- [27] Swartz, E. T., and Pohl, R. O., 1989. “Thermal boundary resistance”. *Review of Modern Physics*, **61**, pp. 605–668.
- [28] Hopkins, P., and Norris, P., 2009. “Relative contributions of inelastic and elastic diffuse phonon scattering to thermal boundary conductance across solid interfaces”. *Journal of Heat Transfer*, **131**, Feb.
- [29] Stevens, R., Zhigilei, L., and Norris, P., 2007. “Effects of temperature and disorder on thermal boundary conductance at solid-solid interfaces: Nonequilibrium molecular dynamics simulations”. *International Journal of Heat and Mass Transfer*, **50**, Apr., pp. 3977–3989.
- [30] Dobbs, E., Figgins, B., and Jones, G., 1958. “Properties of solid argon”. *Il Nuovo Cimento*, **9**.
- [31] Chen, Y. F., Li, D. Y., Yang, J. K., Yu, Y. H., Lukes, J. R., and Majumdar, A., 2004. “Molecular dynamics study of the lattice thermal conductivity of Kr/Ar superlattice nanowires”. *Physica B—Condensed Matter*, **349**(1–4), June, pp. 270–280.

List of Tables

1 Parameters used for the different materials in the simulations [31]. For potentials between different atoms, the energy parameter $\epsilon_{12} = \sqrt{\epsilon_1 \epsilon_2}$ and the length parameter $\sigma_{12} = (\sigma_1 + \sigma_2)/2$ 15

List of Figures

1	Schematic of the interfaces studied via molecular dynamics simulations (From left to right: perfect interface, coarse diffuse interface, fine diffuse interface, single unit cell step interface, hemispherical interface and ellipsoidal interface)	16
2	Verification of solid argon thermal conductivity from molecular dynamics simulations at an average temperature of 50 K	17
3	Temperature distribution in argon system with a length of approximately 7 nm	18
4	Level of rectification of the perfect interface as a function of device length with a fixed temperature difference of 20 K with an average temperature of 50 K from the LAMMPS package	19
5	Amount of rectification in a bulk system as a function of temperature based on fits of experimental measurements of temperature dependent conductivity of argon and krypton.	20
6	Effective rectification of the perfect interface as a function of device length with a fixed temperature difference of 10 K with an average temperature of 10 K from the LAMMPS package	21
7	Level of rectification as a function of device temperature of a system oriented with argon on the left and krypton on the right (ArKr) a system oriented the opposite way (KrAr)	22
8	Level of rectification as a function of device length for perfect and imperfect interfaces from the XMD package	23
9	Level of rectification as a function of device length for asymmetric interfaces from the XMD package . . .	24
10	Level of rectification as a function of temperature for rough interfaces from the LAMMPS package	25

Table 1. Parameters used for the different materials in the simulations [31]. For potentials between different atoms, the energy parameter $\epsilon_{12} = \sqrt{\epsilon_1 \epsilon_2}$ and the length parameter $\sigma_{12} = (\sigma_1 + \sigma_2)/2$

Material	Parameter	Value	Material	Parameter	Value
Kr	ϵ (J)	2.25×10^{-21}	Ar	ϵ (J)	1.67×10^{-21}
	σ (m)	3.65×10^{-10}		σ (m)	3.4×10^{-10}
	a (m)	5.69×10^{-10}		a (m)	5.3×10^{-10}
	m (kg)	1.39×10^{-25}		m (kg)	6.63×10^{-26}
	r_{cut} (m)	9.49×10^{-10}		r_{cut} (m)	8.84×10^{-10}

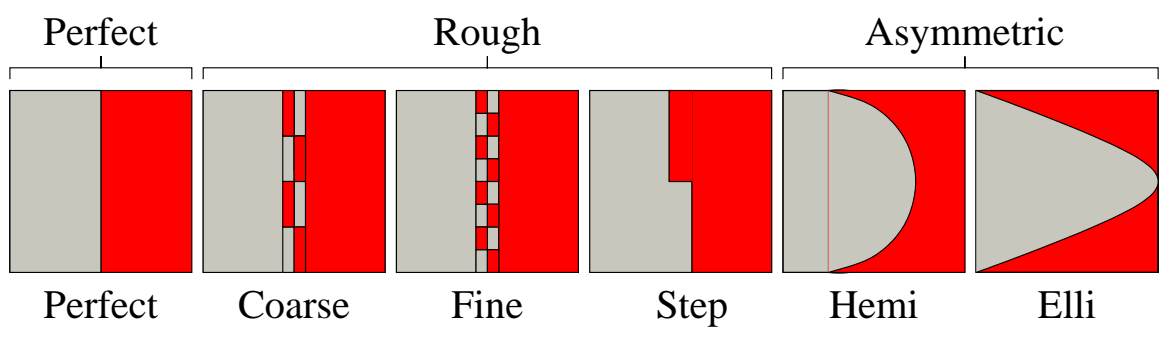


Fig. 1. Schematic of the interfaces studied via molecular dynamics simulations (From left to right: perfect interface, coarse diffuse interface, fine diffuse interface, single unit cell step interface, hemispherical interface and ellipsoidal interface)

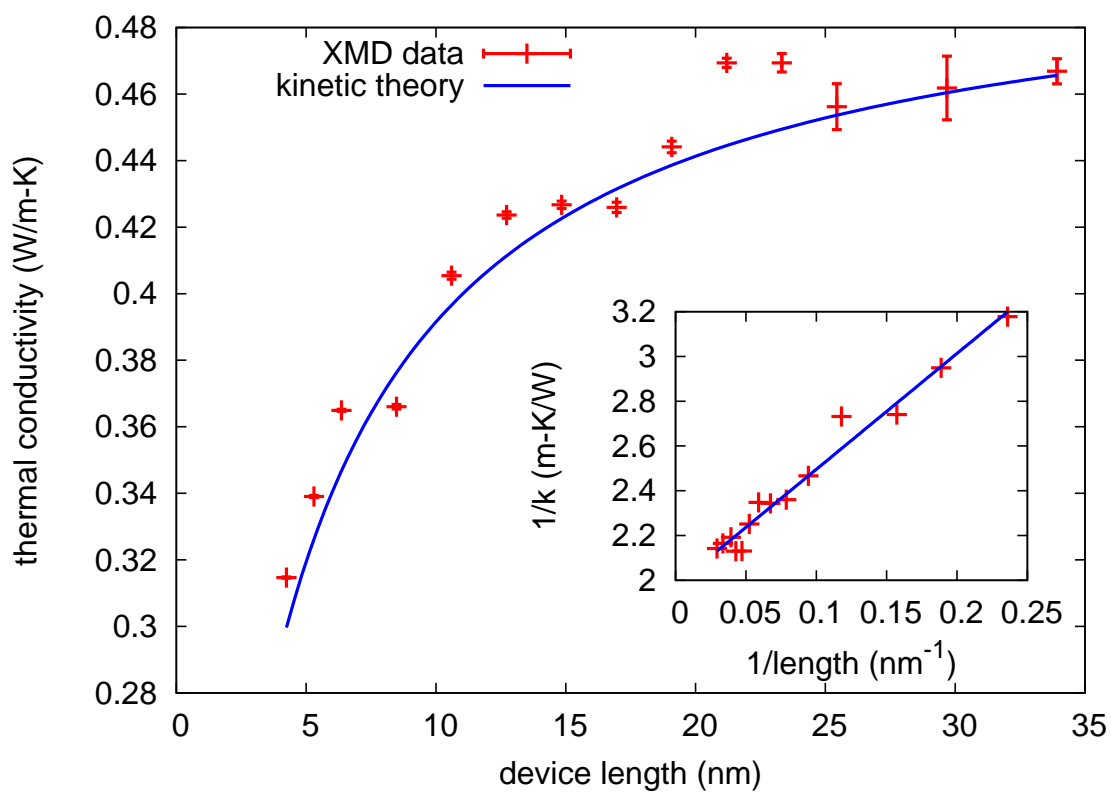


Fig. 2. Verification of solid argon thermal conductivity from molecular dynamics simulations at an average temperature of 50 K

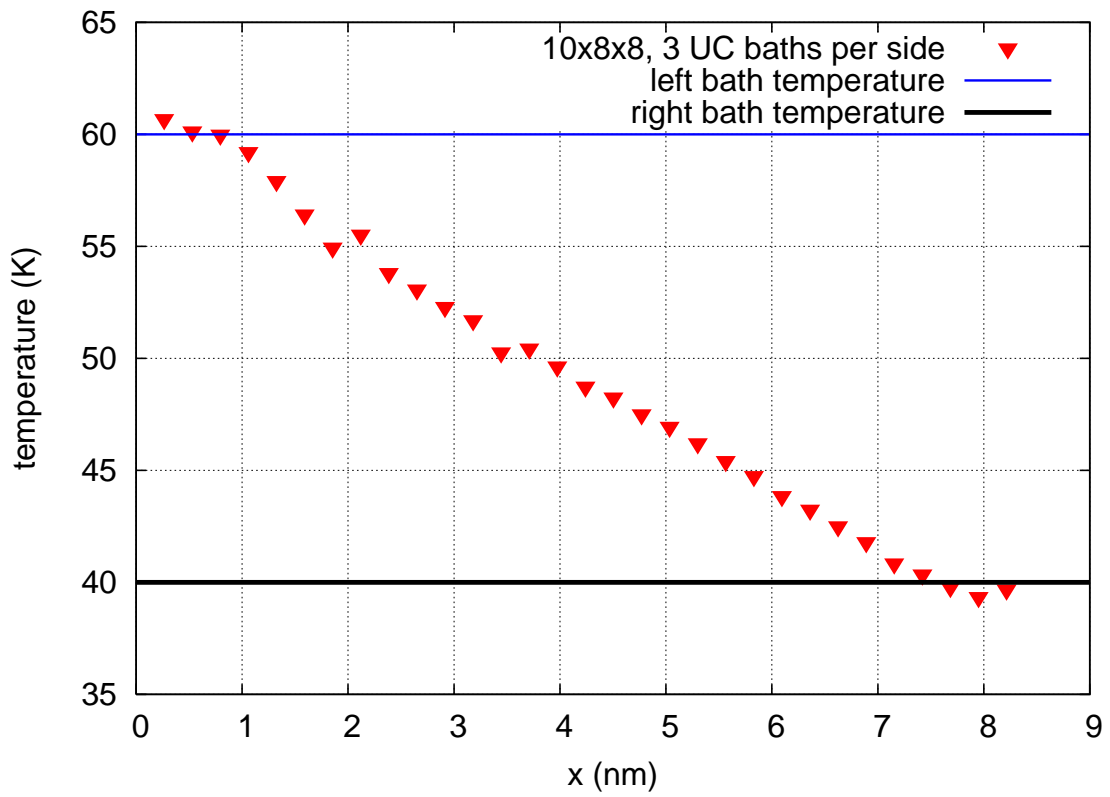


Fig. 3. Temperature distribution in argon system with a length of approximately 7 nm

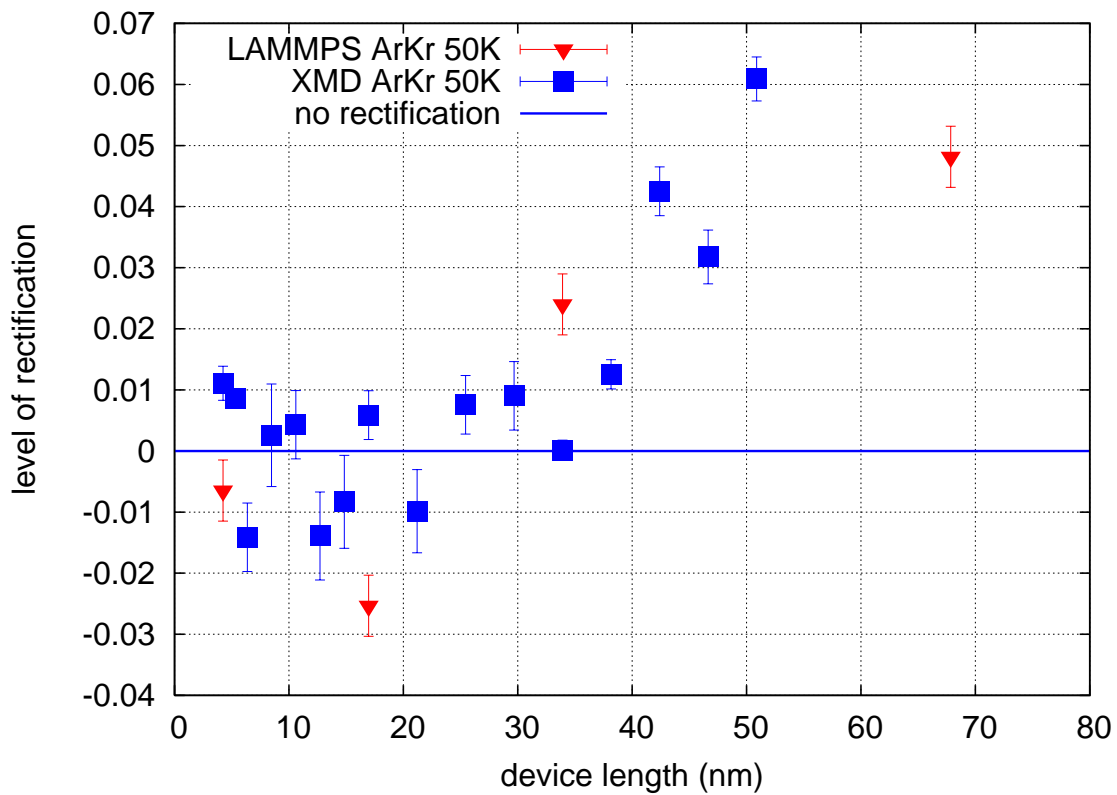


Fig. 4. Level of rectification of the perfect interface as a function of device length with a fixed temperature difference of 20 K with an average temperature of 50 K from the LAMMPS package

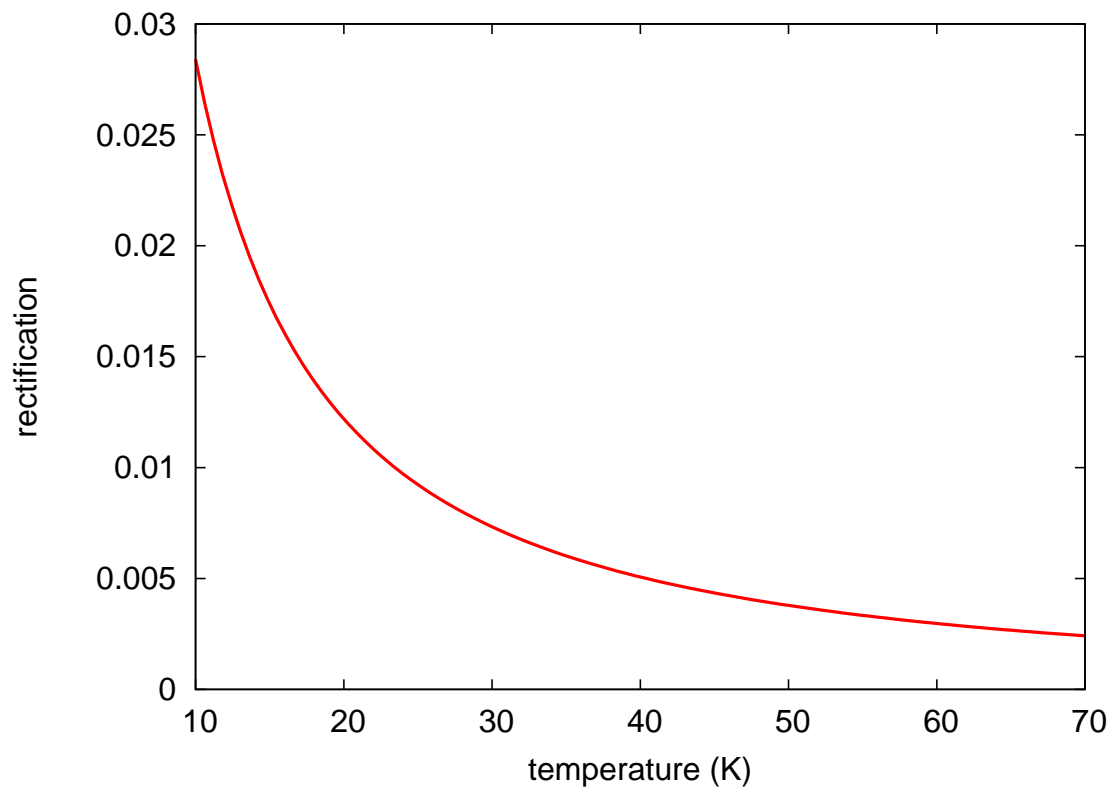


Fig. 5. Amount of rectification in a bulk system as a function of temperature based on fits of experimental measurements of temperature dependent conductivity of argon and krypton.

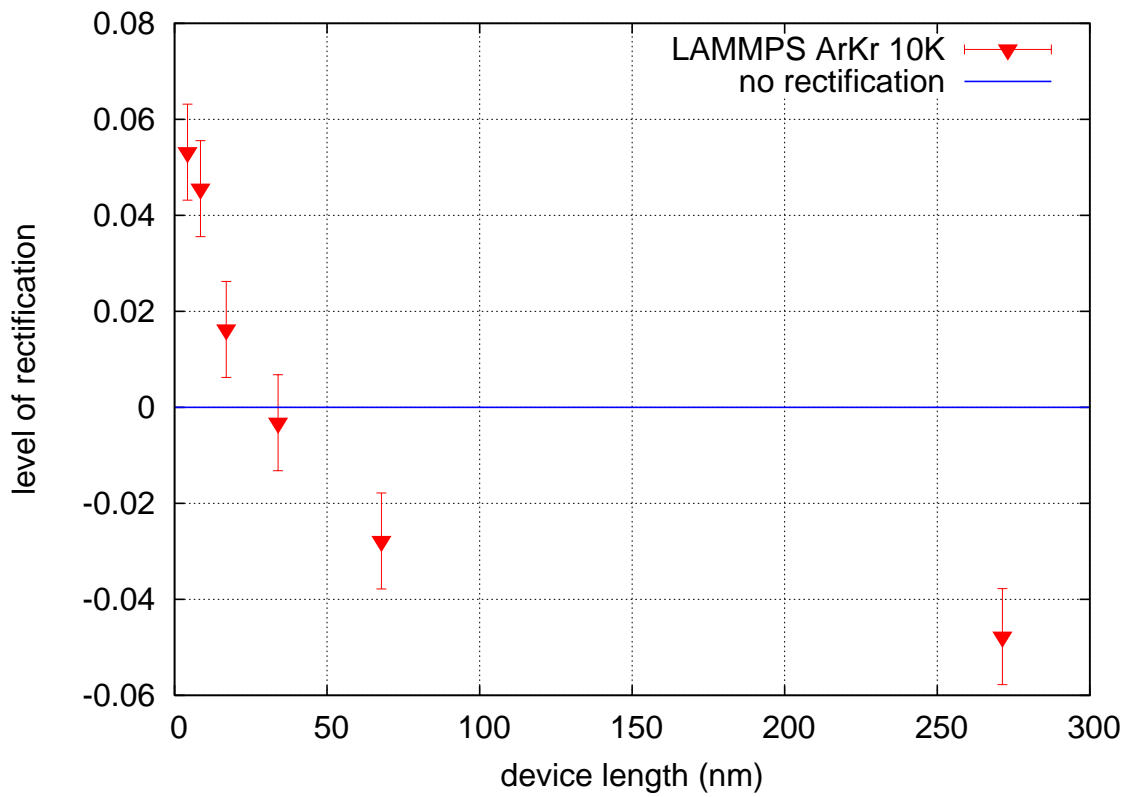


Fig. 6. Effective rectification of the perfect interface as a function of device length with a fixed temperature difference of 10 K with an average temperature of 10 K from the LAMMPS package

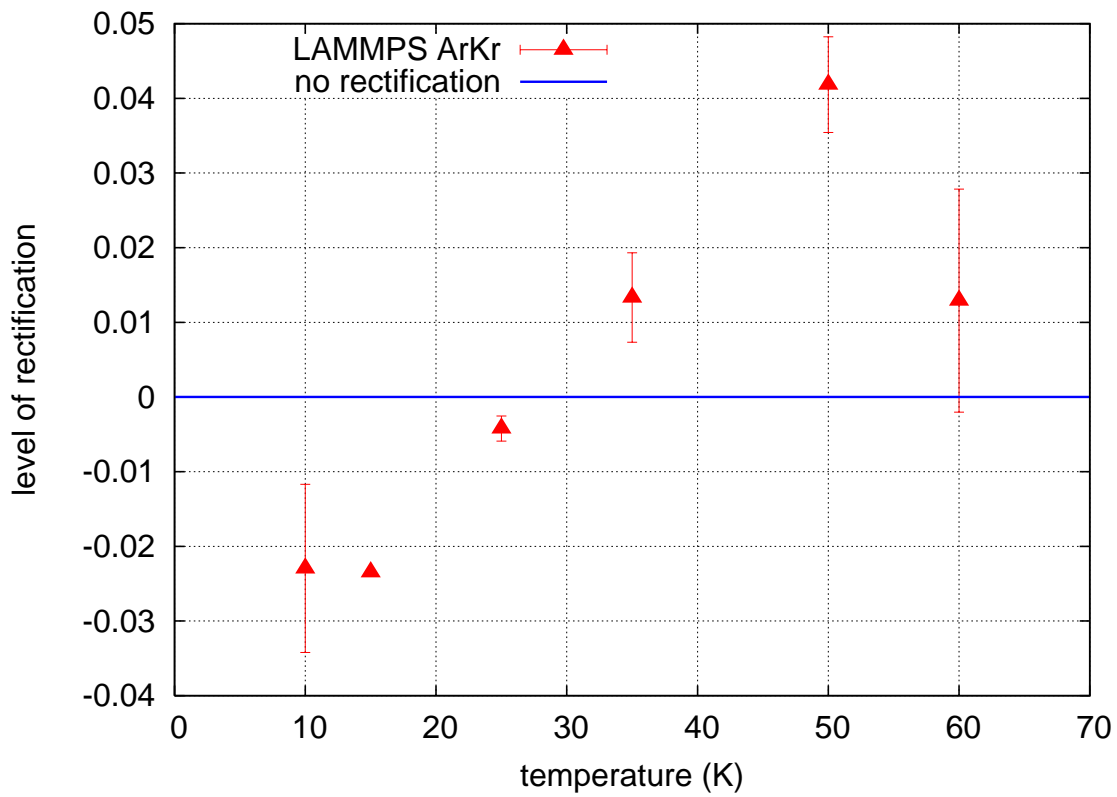


Fig. 7. Level of rectification as a function of device temperature of a system oriented with argon on the left and krypton on the right (ArKr) a system oriented the opposite way (KrAr)

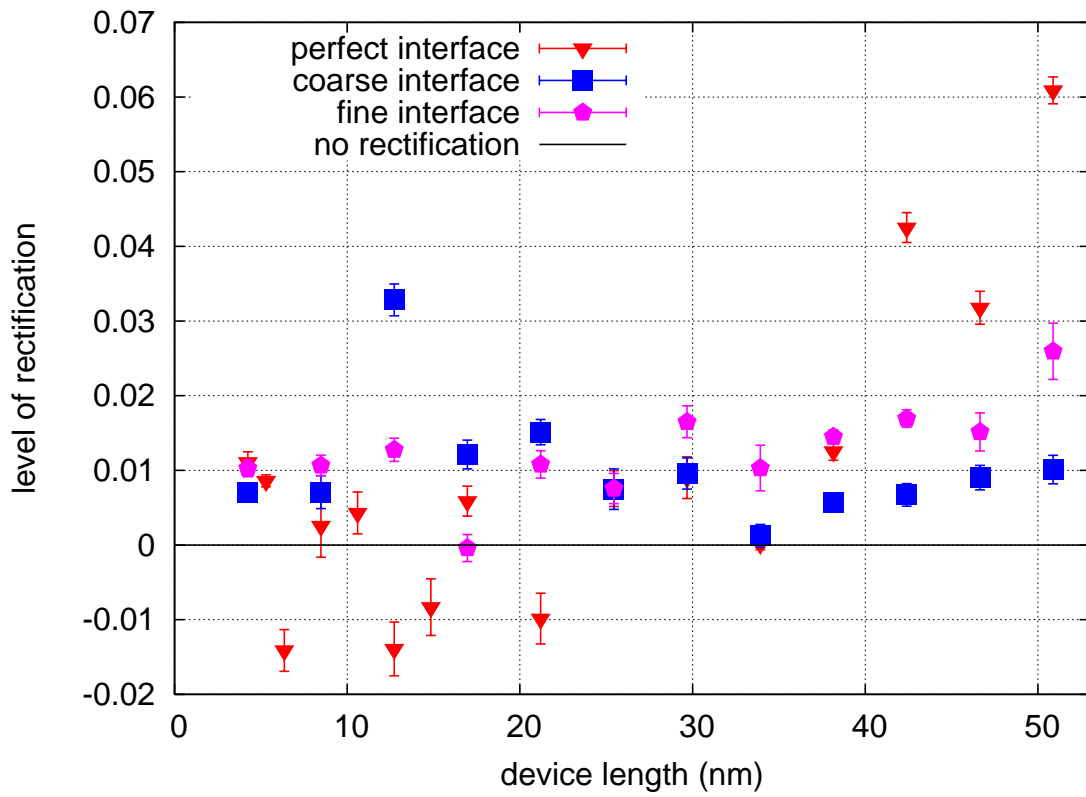


Fig. 8. Level of rectification as a function of device length for perfect and imperfect interfaces from the XMD package

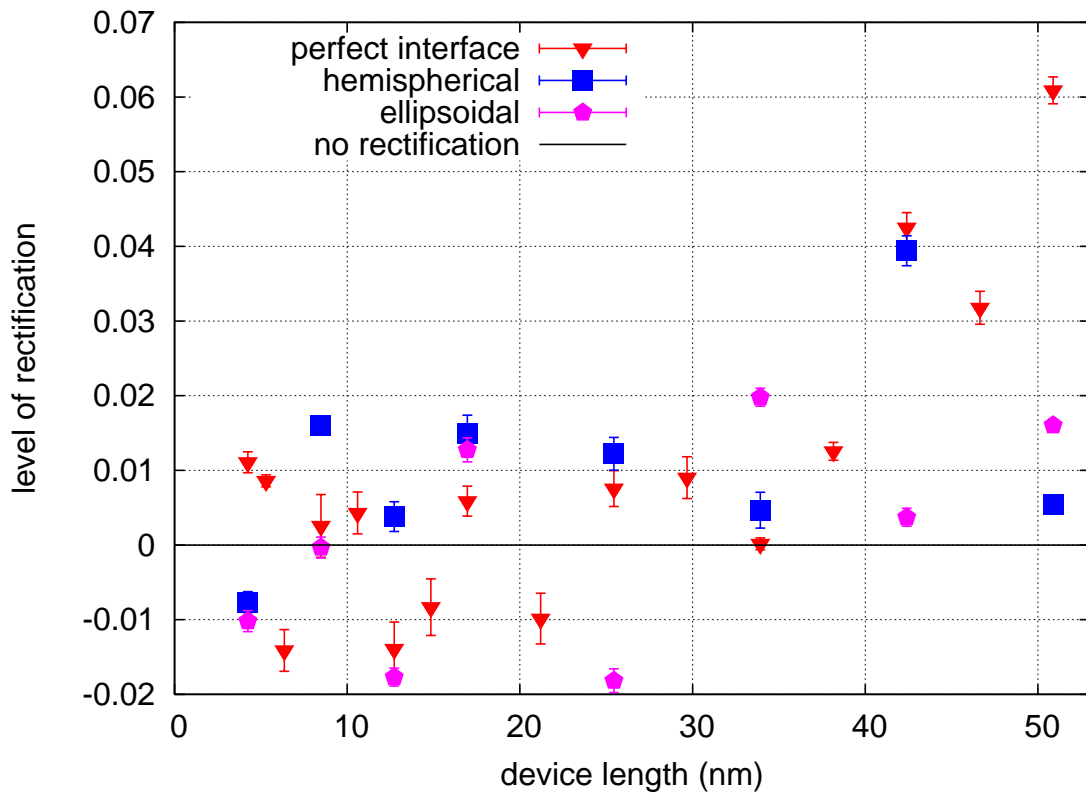


Fig. 9. Level of rectification as a function of device length for asymmetric interfaces from the XMD package

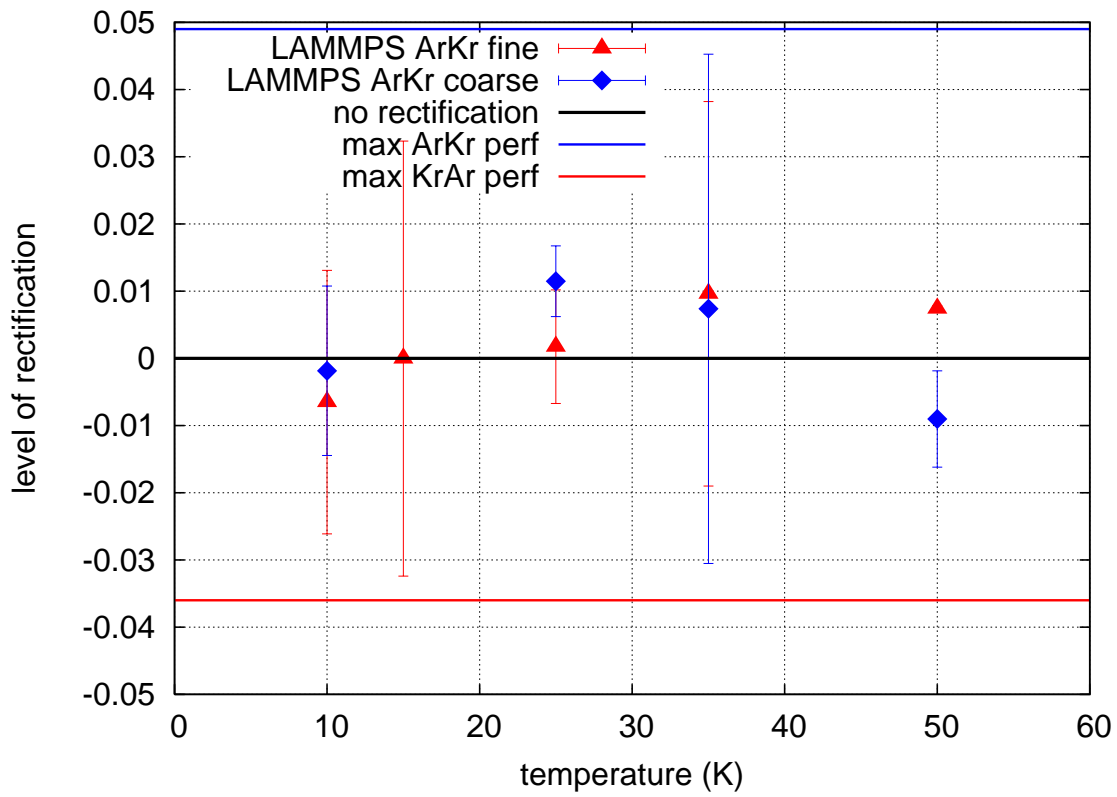


Fig. 10. Level of rectification as a function of temperature for rough interfaces from the LAMMPS package